CVPR #795

Spatiotemporal Contour Tracking of Microtubules

Anonymous CVPR submission
Address Line2
Paper ID 795

Abstract

Microtubules (MTs), one of three major cytoskeletal components, serve numerous critical functions in cells. Mechanistically, MTs are not static polymers; rather, they can be very dynamic and their precise patterns of growing and shortening behaviors are critical to their many functions. Among the challenges confronting modern molecular cell biology is to accurately and thoroughly quantify the dynamic behaviors of cellular MTs under a variety of experimental conditions. MTs in living cells are generally visualized by time-lapse fluorescence microscopy. They appear as thin, hair-like structures, a subset of which are actively changing length. These length changes are generally measured manually. This task is not only laborious but has the potential for inadvertent bias and error. Here, we present a fully automated and robust approach to detect and track MT dynamics that is not only faster than the present manual approach, but it also provides significantly more and higher quality data, which in turn enables novel analyses to be performed. The proposed tracking algorithm addresses issues such as fast growth and shortening of the MTs–often more than 10 pixels from frame to frame, and frequent occlusion and high clutter, using a spatiotemporal contour tracking approach. Experimental results show that highly accurate tracking results can be obtained in a fully automated manner. The output of our tracking method is currently being used in building descriptive mathematical models for capturing the MT dynamics.

1. Introduction

Microtubules (MTs) are cylindrical, cytoskeletal protein polymers found in essentially all eukaryotic cells. They are essential for numerous critical cellular functions, including cell division, various intracellular transport processes, cell movement and cell shape changes. Especially notable among these many functions is the essential role of MTs in separating metaphase chromosomes to the two daughter cells during cell division. Recent work has demonstrated convincingly that proper regulation of the growing and shortening dynamics of MTs is essential in order to achieve proper chromosome segregation (reviewed in [14]). Indeed, the highly effective anti-cancer drug taxol works because it suppresses microtubule dynamics sufficiently to interfere with normal chromosome segregation. Recent work has also suggested that mis-regulation of MT dynamics may underlie Alzheimer's disease and related dementias (reviewed in [8]). Thus, the regulation of MT dynamics is a key element in both normal and pathological cell biology.

Investigators generally visualize MT dynamics using time-lapse fluorescence microscopy. As examples, the images used in this manuscript are taken at 4 second intervals, with about 30-60 frames per stack (i.e., video sequence) of images. Fig. 1 shows an example frame in such a sequence. The image frames have a dimension of 512×600 with a spatial resolution of 1.32 μm per pixel (approximately). The observations that are of interest here include the growth and shortening of these tiny hair-like structures over a period of time. These events occur by addition or loss of monomeric subunits of the MT, known as tubulin.

A typical study of MT characterization would involve imaging the MTs to generate several stacks that are then analyzed to quantify the growth and shortening events. This second step is mostly done manually, by tracking individual microtubule tips, one at a time, over the entire video. From this tip location data, one can then compute statistics such as average growth and shortening. It is fair to say that this is the current state of the art in a typical biology lab (note that there are some recent studies that mark and track MTs using speckle microscopy [5]; however, one can not track the tips alone and tracking the MTs, including their tips, is important in biology.) The obvious problems with such manual analyses include:

- The manual tracking task is time consuming, laborious and subjective. This limits the number of MTs being tracked in a cell to a small number, typically about 5 MTs per video. Hence the complete dynamic behavior of MTs in a cell is not fully captured.
- Only the tip is tracked, leading to inaccurate length estimates when the MT shape is not linear. Besides, since the body of the MT is not captured, no inferences can be

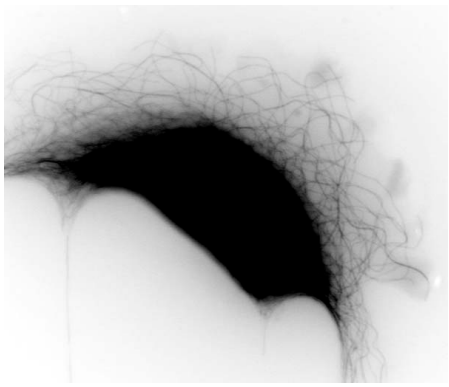

(a)

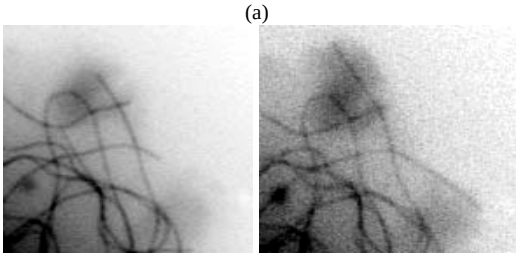

(b) (c)

Figure 1. (a) An example frame of an MT video (b)-(c) A zoom-in on the same area in both frames 4 and 24 of the sequence. The small windows show the high level of noise, and contrast and illumination changes between the two frames. MTs are the hair like structures. (See the supplementary videos)

made about shape changes under different experimental conditions.

The main contribution of this paper is the development of a fully automated method to detect and track MTs in a video sequence. In this work, the MT detection and tracking problems are cast in a novel way as a spatiotemporal graph matching problem. We provide quantitative performance evaluation on MTs with known (manually generated) ground-truth data that support the robustness of the proposed tracking method. More importantly, the detection and tracking further facilitates new analysis that are not currently feasible with the existing manually tracked results. For example, accurate localization of the entire MTs enables shape computations and studying neighboring effects of the MTs in their growth and shortening. To the best of our knowledge, this is the only fully automated method for tracking such structures that can handle occlusions and intersections. The tracking software would be made available on our web site soon.

In the next section we review the related work on microtubule detection and tracking. Sections 3 gives an overview of the proposed tracking technique. Section 4 presents the approach for detecting MT tips. Section 5 details the spatiotemporal matching of MT tips. The MT body formation and experimental results are presented in section 6. Finally, conclusions and future work are discussed in section 7.

2. Related Work

Tracking thin hair like structures such as microtubules, in a noisy microscopy video poses several challenging problems.

- MTs appear as tubular structures in the image frames. The shape of MTs vary within the same cell widely. An accurate estimation of the length of the MT should take into account the curvilinear structure. The currently widely used manual tip tracking and computing the associated statistics ignores this effect.
- MTs undergo large changes in length from frame to frame because of growth or shortening at either MT end. The large change in length, together with frequent occlusions, pose significant problems to any tracking method.
- The images of MTs have low signal-to-noise ratio and exhibit nonuniform illumination both spatially and temporally.

Our contributions directly address the above issues. In reviewing the related work, we first provide an overview of the state-of-the-art in MT tracking and discuss tracking related research as applicable to our proposed methodology.

2.1. Microtubule detection and tracking

In the literature few papers [3, 4, 6, 10, 12, 13] have addressed the MT detection and tracking problems. In [4], a graph searching algorithm is applied to manually selected microtubule ending points, and the shortest path is computed to extract the central axis of the microtubule. In [12], the authors propose to automate the microtubule segmentation by extending the active shape model using a higher order boundary model, and Kalman filtering to utilize the shape information along the longitudinal direction of the MTs. In [13], the authors propose an automated approach to extract the microtubule tip with a coarse to fine scale scheme consisting of volume enhancement and tip segmentation. In [10], the microtubules are extracted in terms of consecutive segments by solving Hamilton-Jacobi equations. The algorithm extracts the microtubule starting from a manually selected tip. All of the above methods have only addressed the MT detection problem without handling the tracking of MTs.

In [6], an initial point is selected on a microtubule and iteratively gives a stack of points representing the microtubule using tangent constraints. Once the microtubule is detected, it is tracked in time while constraining the search space in a normal direction around microtubule points. Though the tracking algorithm is automated, the authors report difficulties in handling MT intersections and do not present quantitative tip tracking performance results. The main issue with their approach is that MT tracking is performed using a local measure of consistency that can lead to

problems at intersection. In this work, we propose a global multiframe approach to resolve tracking conflicts. The work in [3] presents a framework for detecting and tracking images of linear structures in differential interference contrast (DIC) microscopy. The tracking of the movements of MT segments is performed using a sum of squared (brightness) differences algorithm based on an initial manual input.

2.2. Detection and Tracking of Curvilinear structures

Curvilinear structures detection and tracking represent important computer vision problems for applications such as road detection, mammographic image analysis, fiber identification, fingerprint image analysis, and MTs and actin filaments identification. Many techniques have been proposed in the literature to detect curvilinear structures such as scale space approaches with Gaussian derivatives [17], anisotropic Gauss filtering [9], fusion of two local line detectors followed by a global Markov random field [25], and using differential geometric properties of images [23]. For the problem of correspondence of curvilinear structures between sets of images, algorithms have been proposed in the literature for applications such as tracking and 3D reconstruction. In the majority of approaches, lines are first detected and then line properties such as orientation, position, width and center lines are used for the matching process [15, 18].

In all of these techniques, a threshold is used to binarize the line detector response prior to matching between the images. In real life noisy video sequences, it is very likely that the required threshold will vary from frame to frame, thus causing a possible loss of the tracked curvilinear structure. Instead of tracking using the binarized response, we propose to use an active contour framework that uses the continuous line detector response to detect and track the curvilinear structures.

2.3. Active contour tracking approaches

Active contours are curves deforming in the image plane according to image features and internal smoothness constraints. They have been used previously for object tracking applications. We will classify these approaches based on two features: 1) explicit motion estimation to predict object position from frame to frame, and 2) capability to handle the multi-objects.

The simplest case is when a single object/region is tracked without any motion estimation [20, 24]. The second class uses motion estimation technique for tracking a single region [1, 2]. The third category handles explicitly the multi-object case but does not use motion estimation assuming high enough frame rate giving small displacements from frame to frame [11, 19]. The last class uses motion estimation and is addressing the issue of tracking interacting objects as in [7]. Since we are concerned with tracking multiple MTs in a video with large interframe changes, our proposed method falls into the last category of contour tracking. However, we use a multiframe motion estimation that can resolve tracking conflicts in a more systematic fashion.

3. Overview of the approach

We model a microtubule in a video frame as an open curve $C(s)$ where $s \epsilon [0, 1]$ is the curve parameter (see fig. 2). Due to the highly dynamic nature of MTs and their frequent intersections, a spatiotemporal tracking algorithm based on deformable contours is an effective strategy. We propose to use an active contour based on line features to capture deformations of the microtubule in a given frame. The active contour is an open curve in this case with one end fixed and the other - the tip- is free to move.

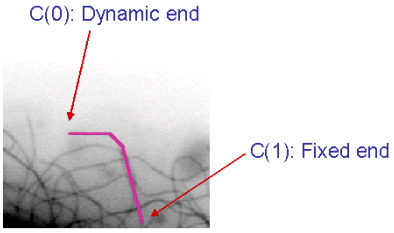

Figure 2. MT model as an open curve with only one moving end (the tip) superimposed on a video frame .

Since, the MT tip can be changing its location in every frame, we need to estimate the motion of the tip. We proceed to detect the tips in a given frame and match tips between subsequent frames that belong to the same MT. Hence, the main modules of the proposed tracking approach shown in fig. 3 are:

- *Tip detection*: Given a MT video, we design a tip detector generating the locations of MT tips in every frame. Note that the number of the detected tips in every frame need not to be equal.
- *Multiframe tip matching to generate tracks*: Given the detected tips in every frame, we need to match tips between frames to form MT tracks. We formulate this problem as a graph matching one, by considering all tips from all the frames simultaneously. The advantage of spatiotemporal matching of tips is that it enforces continuity of tracks, and is able to handle missing tips in some frames due to noise and to discard false positives.
- *Extracting MT bodies*: We propose an active contour-based approach to track the full body of the microtubule based on the tip locations in a given microtubule track. Being able to track changes in the full body of the MT instead of just the tip location enables a better estimate of the MT length. Furthermore, we can now study shape changes in MTs which can not be performed based on

tip tracking only.

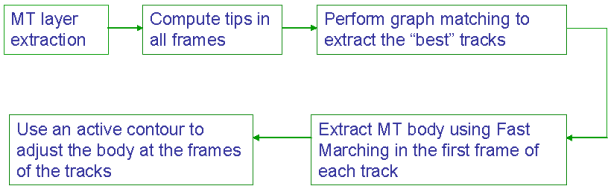

Figure 3. The block diagram of the proposed tracking technique.

4. Microtubule Tip Detection

Given a video frame, MT tips are detected which will be tracked subsequently. We are usually interested in MTs growing or shortening near the cell membrane. We first extract a band around the cell membrane -the MT layer- through temporal clustering in the frequency domain.

4.1. Extracting MT layer by temporal clustering

A microtubule video of T frames can be considered as a spatiotemporal volume. At each pixel location (x, y) on the first frame, we construct a vector $F(x, y)$ in the time direction, thus it will have a dimensionality of T. We construct a feature vector from $F(x, y)$ by taking the FFT. The motivation behind using a frequency based representation of the volume is to partition the MT video into regions of different spatial activity patterns. We retain the magnitudes of the coefficients only. We discard the DC component for intensity invariance and take the first half of the FFT coefficients. We end up representing the whole video volume by FFT vectors. We then cluster these FFT vectors using a K-means algorithm into V clusters corresponding to regions of varying activity in the cell. Finally, we extract the clusters corresponding to the region of highest activity, which we call the microtubule layer. An example of the extraction of the microtubule layer is shown in fig. 4.

4.2. Ridge-based detection of MT

After extracting the MT layer, a filtering approach is used to detect the MT tips in this layer. Our algorithm for tip detection starts by extracting a binary mask showing the locations of microtubule polymer. The basic assumption about MTs that enables extracting a binary mask of microtubule locations is that MTs look like black curvilinear structures on a light background in an ideal scenario. A second derivative of Gaussian kernel matched to image locations at different orientations should reveal this tubular structure while eliminating background noise. Let the intensity function in the window of interest W be denoted as I_W, the output after filtering the window is then:

$$I^f_W(x, y) = \max_\theta(I_W(x, y) * G''_{\sigma,\theta}(x, y)) \qquad (1)$$

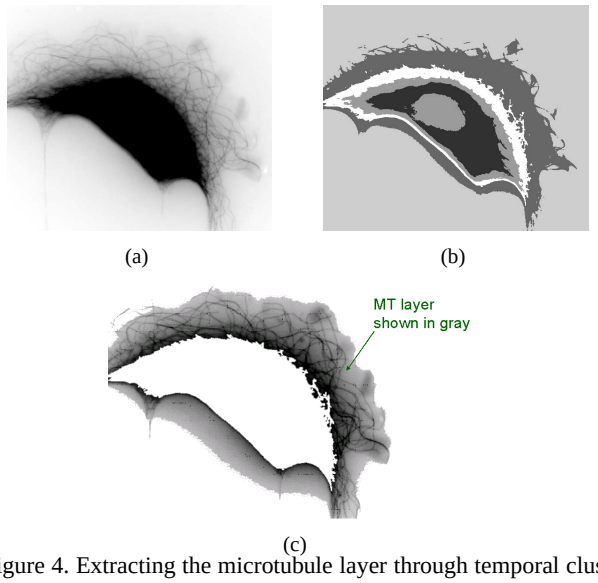

Figure 4. Extracting the microtubule layer through temporal clustering. (a) One of the image frames from the video, (b)K-means clustering into 5 clusters including one for the background and (c) The region of the frame corresponding to the microtubule layer. (other parts are shown in white)

where $G''_{\sigma,\theta}(x, y)$ is a second derivative of Gaussian kernel with scale σ and orientation θ at position (x, y). σ is chosen experimentally based on the microtubule width. An example of finding the maximum of a second derivative of Gaussian convolved with the image at all pixel locations is shown in Fig 5.

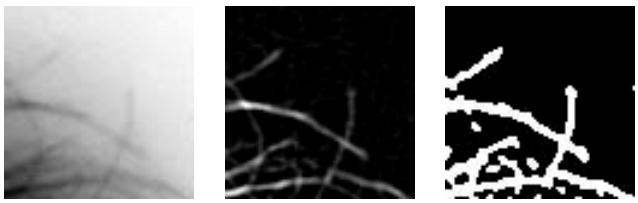

Figure 5. A window I_W in a video frame, (b) the filter output I^f_W and (c) binarization.

4.3. Detecting MT Tips

The binary MT mask computed based on second derivative of Gaussian filtering is thinned to generate one pixel width lines. A test is performed at every white pixel location to check if the pixel is a line ending. Mimicking the manual method to select MT tips that are free of too much clutter, we filter out tips that are in locations where the ratio of MT polymer to non-polymer masses is less than a threshold - we take it 0.3 experimentally. An example of MT tip detection is shown in figure 6.

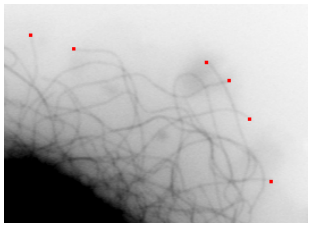

Figure 6. An example of MT tip detection in a frame.

5. Spatiotemporal tip matching

Having generated a set of tips in every frame of the MT video, we seek to match corresponding tips between frames to form MT tracks. One possibility is to track tips from frame to frame. However, due to the low signal to noise ratio in the images, this is likely to fail. Instead, we consider matching tips from all the frames directly in a spatiotemporal manner. The main advantages of this approach are:

- It can handle missing tips due to noisy conditions by allowing the final MT tracks to skip frames in between.
- It can potentially remove spurious tips found if the noise/ loss in signal does not occur repeatedly at nearby locations.

At the end of the tip matching over all the frames, we can select the longest tracks for further processing, since short tracks are likely to be due to noise. It is worth noting that the computed tracks in this manner can start and end at any given frame of the video sequence, can have arbitrary lengths, and can be skipping frames in the middle. We formulate the problem of tip matching as a graph matching one.

5.1. Graph-based Formulation

Consider an MT video of length T frames. Let us denote N_i to be the number of tips detected in frame i for $1 \leq i \leq T$. Denote the tip detected in a frame as t_i^h with the subscript corresponding to the frame number and the superscript corresponding to the tip number in frame f_i, thus h has the range $1 \leq h \leq N_i$. We construct a graph $G = (V, E)$ whose vertices V correspond to the detected tips in every frame and the edges E represent similarity between vertices. The edge weights of the graph represent the matching gain of corresponding two tips in different frames. In order to allow MT tracks to skip some frames, we include edges between tips in non-consecutive video frames. An example of a graph used for tracking MTs is shown in fig. 7 with a possible solution of tip matching.

5.2. Similarity metric proposed

The main metric which defines the matching of tips for the video frame is the similarity measure linking tips in different frames. Consider two tips t_i^h and t_j^r in two separate

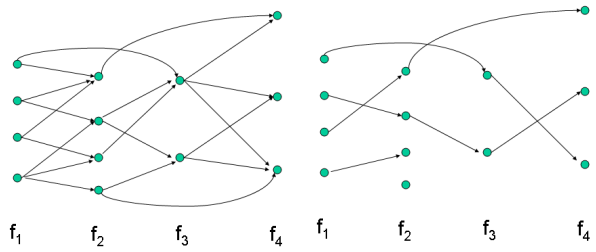

(a) (b)

Figure 7. (a) An example graph whose vertices are the tips detected in every frame of video (here shown for a length 4 video) and (b) a possible maximal matching solution. Note that the tracks can be of different lengths, start and end at arbitrary frames, and skip frames in between.

frames f_i and f_j. For example, one can use:

$$Sim(t_i^h, t_j^r) = \frac{1}{1 + d(t_i^h, t_j^r)} \quad (2)$$

where $d(.,.)$ is the Euclidean distance. However this will have problems in cases of tips of different MTs coming close to each other. A better alternative is to consider a distance constrained on the MT body, such as a geodesic distance. We consider the cases of growth and shortening of an MT between two different frames as in Fig. 8. For the MT growth, we project the location of the tip on frame f_i to the same location on frame f_j. We then compute the first geodesic distance $d_{geod_1}(t_i^h, t_j^r)$ as shown on Fig.8. For the MT shortening case, we back-project the location of the tip on frame f_j to the same location on frame f_i. We then compute the second geodesic distance $d_{geod_2}(t_i^h, t_j^r)$ as shown on Fig.8. Note that, for a given MT, we do not have a-priori information on whether it is growing or shortening. Finally the similarity metric -edge weight on the graph G - used between the two tips t_i^h and t_j^r is computed as follows:

$$Sim(t_i^h, t_j^r) = e^{-min(d_{geod_1}, d_{geod_2})} \quad (3)$$

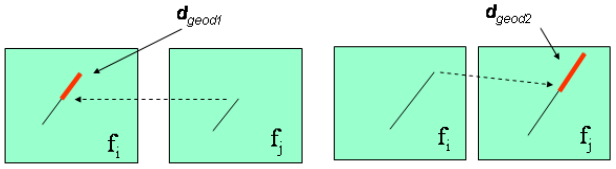

(a) (b)

Figure 8. Illustration on how the similarity weight between vertices of the graph is computed between tips in two different frames f_i and f_j (see text for explanation). (a) case of shortening and (b) case of growing.

5.3. Maximum matching on the graph

Given the graph G of MT tips as vertices and the edge weights as defined in (3), we compute a maximum weight

matching of the tips which correspond to MT tracks. From graph theory, we know that a *vertex disjoint path cover* C is a covering of G where each vertex of G is in some path of C and each vertex belongs to one path only. The weight of a path cover is the sum of weights of edges on the path cover. Given an initial graph G, the problem of finding the best MT tracks corresponds to finding the *maximum weight path cover* of G with the weights defined by the similarity in (3). Formally, a maximum weight path cover $C(G)$ is a path cover which satisfies:

$$C(G) = \arg\max_{C_i} W(C_i) \tag{4}$$

where $W(C_i) = \sum_{e_{uv} \epsilon C_i} Sim(e_{uv})$ and u, v are two vertices in G for which the similarity is computed as in (3).

We proceed to compute the maximum weight path cover as suggested in [22]. Let us define a split graph G_{split} corresponding to G as a bipartite graph with partite vertix sets V_+ and V_-. V_+ and V_- are copies of the vertices V. An edge e_{uv} between two vertices u and v in G has the same weight as the edge $e_{u_+v_-}$ in G_{split}. The edges of maximum matching of the bipartite split graph G_{split} correspond to the edges of maximum path cover of G.

6. MT body formation based on geodesics

After computing the maximum weight match for the constructed graph of tips, we can use the MT tracks formed by the matched tips to compute dynamic parameters of importance of MTs such as growth and shortening rates. However, the MT length estimation based on tip location only is inaccurate when the body of the MT is not linear or in case of lateral motion. A better alternative would be to extract the MT body and use it in the computation of the MT length. Furthermore, we can study the effect of different experimental subjects on the curvature of the MT, which was not possible before. Consider for example an extracted MT track with a starting frame f_k. We proceed as follows to compute the MT body in the first frame f_k of this track.

Denoting the location MT tip of interest as t_{start}, the goal is to find a point t_{end} on the MT to form the body. For this purpose, let us define first the set P of points satisfying:

$$P = \{t_i \forall (\int_{t_{start}}^{t_i} I_W^f(s) ds) < \xi\} \tag{5}$$

where $I_W^f(.)$ is as defined in (1). In other words, the set of points P is the one for which the geodesic distance from the tip t_{start} is below the threshold ξ determined experimentally. Using the set P, we define t_{end} which maximizes the following:

$$t_{end} = \arg\max_{cand \in P} \|t_{start} - t_{cand}\|^2 \tag{6}$$

This is equivalent of finding the path with minimum curvature originating from the tip. We then use a gradient descent to trace the MT body from the tip to the ending point determined on the MT. The procedure of tracing the MT body is depicted in fig. 9. Note that we consider the ending point on the MT to be fixed along the MT track for the remaining frames. For subsequent frames, the problem of extracting the MT body is thus transformed into deforming the body between the fixed ending point and the tip detected using the spatiotemporal matching. The deformation of the MT body is carried out using an active contour method based on line features, as explained below.

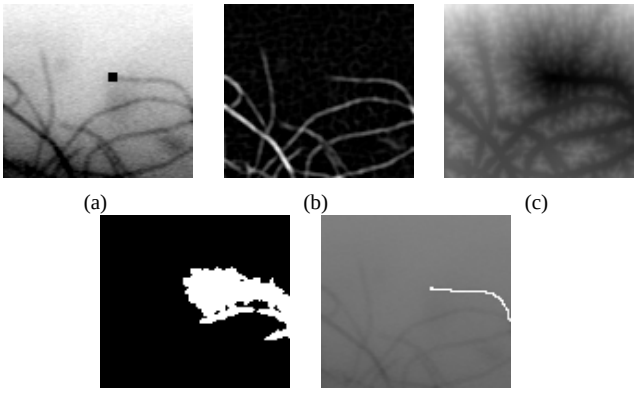

Figure 9. MT body formation in the first frame of a track (a) A window around the considered tip in the track with tip overlaid as a black square on the window, (b) The filtering result of the window used as an input to the geodesic distance transform, (c) The distance transform from the tip with darker values denoting smaller distances, (d) points satisfying a distance threshold less than 1, (e) The extracted MT body.

6.1. Active contour for MT deformation

"Snakes" are deformable contours that are initialized on the image plane and allowed to evolve under the influence of a set of internal and external forces. Let the contour be represented parametrically as $C(s)$ where $s \epsilon [0, 1]$, an energy functional that needs to be minimized is defined as follows:

$$E(C(s)) = \int_0^1 (E_{\text{int}}(C(s)) + E_{ext}(C(s)))\, ds \tag{7}$$

where $E_{\text{int}}(C(s))$ is the internal snake force composed of a balanced weight of tension and rigidity of the contour. Since we are interested in tracking MTs that appear as curvilinear structures in an image $I(x, y)$, we use *ridge* (accordingly *valleys*) features as the external force $E_{ext}(C(s))$. Ridge features can be detected using a second order derivative of a Gaussian $G''_\sigma(x, y)$. Consider the following exter-

CVPR #795

MT Video	# MTs	μ_{error}	σ_{error}
1	10	2.25	2.64
2	16	2.85	4.36

Table 1. MT tip tracking performance. The duration of the MT video tracks is 25 frames.

nal force:

$$\nabla E_{ext} = w_1 \left(-\nabla L\right) + w_2 \, L \, sign(\langle -\nabla L, \vec{N} \rangle) \, \vec{N} \quad (8)$$

where the first term:

$$-\nabla L(x,y) = -\nabla \frac{1}{1 + |G''_\sigma(x,y) * I(x,y)|^2}$$

is a gradient vector field created from the line detector response $|G''_\sigma(x,y) * I(x,y)|$. The purpose of this vector field is to pull the active contour towards the desired curvilinear structure of the MT. The second term $L.sign(\langle -\nabla L, \vec{N} \rangle).\vec{N}$ is a balloon-based term used to speed convergence of the contour and to help moving the contour in smooth areas (with the sign term inspired by the work of [16]).

6.2. Tracking Results and Quantitative Performance Evaluation

We have applied our automated tracking algorithm on 250 MT videos, generating on average 20-25 MT tracks per video. In our implementation of the spatiotemporal graph matching, we allowed up to three missing frames between tips of the same MT track. For the computation of the geodesics, we used the Fast Marching algorithm [21]. The complete tracking of MTs within a video of 30 frames takes approximately 30 minutes using a Matlab implementation on a 3 GHz P-IV machine with 1G RAM. fig. 10 and 11 show example results on some of the frames. Note that there are three generated MT tracks one for each of the MTs in fig. 10. More results are supplemented as videos with the paper submission. To evaluate the tracking performance of MTs, we manually tracked MT tips in two video sequences. The tip tracking performance is shown in table 1. The average MT track duration in these videos is 25 frames.

The computed errors appear very reasonable and acceptable for further manual/computer analysis. As we mentioned before, there are no currently publicly available methods and datasets where such a performance has been documented. We plan to provide on the Internet both the datasets (with known MT trajectories) as well as our software implementation for use by other researchers.

7. Conclusions

We have presented in this paper a novel, fully automated, tracking technique for MTs. The technique is based on a spatio-temporal contour tracking approach that can handle missing features and resolve tracking conflicts. For the first time in the published literature, we presented quantitative evaluation of the tracking performance for a set of manually tracked MTs. By generating a large number of full-body MT tracks, very useful and previously non-acquirable data can be harvested. Example applications include: 1) Quantifying the effect of different experimental conditions on MT shape since we have full body tracking, and 2) Modeling the full time series of the MT tracks using statistical tools to better understand the underlying cell mechanisms regulating MT behavior.

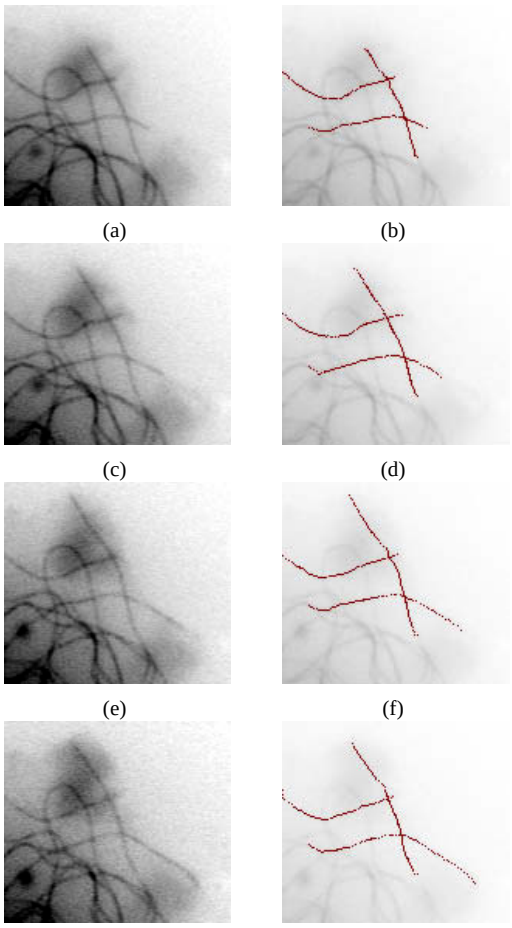

Figure 10. Example frames (5,12,18, and 27) from automatically computed MT tracks.

References

[1] V. Caselles and B. Coll. Snakes in movement. *SIAM Journal on Numerical Analysis*, 33(6):2445–2456, 1996.

[2] M. Castaud, M. Barlaud, and G. Aubert. Tracking video objects using active contours. In *Proceedings. Workshop on Motion and Video Computing*, pages 90–95, Dec. 2002.

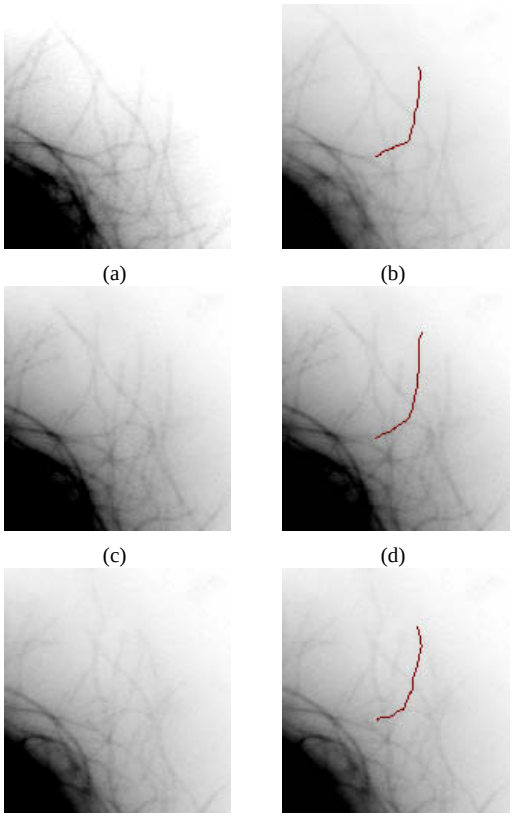

Figure 11. Example frames (9,14, and 19) from automatically computed MT tracks.

[3] G. Danuser, P. Tran, and E. Salmon. Tracking differential interference contrast diffraction line images with nanometre sensitivity. *Journal of Microscopy, 198*, pages 34–53.

[4] L. L. et al. Extraction of 3d microtubules axes from cellular electron tomography images. In *Proc. of ICPR*, volume 1, pages 804–807, 2002.

[5] P. V. et al. Tracking retrograde flow in keratocytes: News from the front. *Molecular Cell Biology*, 16:1223–1231.

[6] S. H. et al. Automatic quantification of microtubule dynamics. In *Proc. of Int. Symp. on Biomedical Imaging: From Nano to Macro*, 2004.

[7] Z. K. et al. A system for tracking laboratory animals based on optical flow and active contours. In *International Conference on Image Analysis and Processing*, pages 334–339, Sept. 2001.

[8] S. Feinstein and L. Wilson. Inability of tau to properly regulate neuronal microtubule dynamics: a loss-of-function mechanism by which tau might mediate neuronal cell death. *Biochim Biophys Acta*, 36(2):268–79, Jan 2005.

[9] J. Geusebroek, A. Smeulders, and J. van de Weijer. Fast anisotropic gauss filtering. *IEEE Transactions on Image Processing*, 12(8):938–943, Aug 2003.

[10] S. Hadjidemetriou, D. Toomre, and J. S. Duncan. Segmentation and 3d reconstruction of microtubules in total internal reflection fluorescence microscopy (tirfm). In *8th International Conference on Medical Image Computing and Computer Assisted Intervention, (MICCAI)*, 2005.

[11] R. Hsu and A. K. Jain. Generating discriminating cartoon faces using interacting snakes. *IEEE Transactions on Pattern Analysis and Machine Intelligence*, 25(11):1388–1398, Nov. 2003.

[12] M. Jiang, Q. Ji, and B. F. McEwen. Model-based automated segmentation of kinetochore microtubule from electron tomography. In *Proc. of 26th Annual International Conference of the Engineering in Medicine and Biology Society*, 2004.

[13] M. Jiang, Q. Ji, and B. F. McEwen. Automated extraction of microtubules and their plus-ends. In *WACV/MOTION 2005*, pages 336–341, 2005.

[14] M. Jordan and L. Wilson. Microtbules as a target for anticancer drugs. *Nature reviews, Cancer*, 4:253–265, Apr 2004.

[15] B. Kamgar-Parsi. Algorithms for matching 3d line sets. *IEEE Transactions on Pattern Analysis and Machine Intelligence*, 26(5):582–593, May 2004.

[16] R. Kimmel and A. Bruckstein. Regularized laplacian zero crossings as optimal edge integrators. *International Journal of Computer Vision*, 53(3):225–243, 2003.

[17] T. Lindeberg. Edge detection and ridge detection with automatic scale selection. In *Computer Vision and Pattern Recognition*, pages 465–470, June 1996.

[18] R. Marti, R. Zwiggelaar, and C. Rubin. Tracking mammographic structures over time. In *British machine vision conference*, 2001.

[19] D. Mukherjee, N. Ray, and S. Acton. Level set analysis for leukocyte detection and tracking. *IEEE Transactions on Medical Imaging*, 13(4):562–572, April 2004.

[20] N. Paragios and R. Deriche. Geodesic active contours and level sets for the detection and tracking of moving objects. *IEEE Transactions on Pattern Analysis and Machine Intelligence*, 22(3):266–280, March 2000.

[21] J. Sethian. *Level Set Methods and Fast Marching Methods*. Cambridge Univ. Press, 1999.

[22] K. Shafique and M. Shah. A noniterative greedy algorithm for multiframe point correspondence. *IEEE Transactions on Pattern Analysis and Machine Intelligence*, 27(1):51–65, Jan 2005.

[23] C. Steger. An unbiased detector of curvilinear structures. *IEEE Transactions on Pattern Analysis and Machine Intelligence*, 20(2):113–125, Feb 1998.

[24] J. Tang and S. T. Acton. Vessel boundary tracking for intravital microscopy via multiscale gradient vector flow snakes. *IEEE Transactions on Biomedical Engineering*, 51(2):316–324, Feb 2004.

[25] F. Tupin, H. Maitre, J. Mangin, J. Nicolas, and E. Pechersky. Detection of linear features in sar images: application to road network extraction. *IEEE Transactions on Geoscience and Remote Sensing*, 36(2):434–453, Mar 1998.